FULL PAPER

Dalton
www.rsc.org/dalton

Organometallic β-turn mimetics. A structural and spectroscopic study of inter-strand hydrogen bonding in ferrocene and cobaltocenium conjugates of amino acids and dipeptides †

Dave R. van Staveren,[a,b] Thomas Weyhermüller[a] and Nils Metzler-Nolte*[b]

[a] *Max-Planck-Institut für Strahlenchemie, Stiftstraße 34-36, D-45470 Mülheim/Ruhr, Germany*

[b] *Institut für Pharmazie und Molekulare Biotechnologie, Universität Heidelberg, Im Neuenheimer Feld 364, D-69120 Heidelberg, Germany. E-mail: Nils.Metzler-Nolte@urz.uni-heidelberg.de*

Received 28th August 2002, Accepted 20th November 2002
First published as an Advance Article on the web 9th December 2002

By using organometallic turn-mimetics, we have investigated the influence of a positive charge on the structure and stability of peptide turn structures which are stabilized by hydrogen bonds. Starting from metallocene mono- (**1**) or di-carboxylic acid (**2**), 11 amide derivatives were prepared, namely $CpMC_5H_4$-CO-Phe-OMe (**3**), $CpMC_5H_4$-CO-Ala-Phe-OMe (**4**), $CpMC_5H_4$-CO-NH-CH(CH_3)-Ph (**5**), $M(C_5H_4$-CO-Phe-OMe$)_2$ (**6**), $M(C_5H_4$-CO-Ala-Phe-OMe$)_2$ (**7**), and $Fe(C_5H_4$-CO-NH-CH(CH_3)-Ph$)_2$ (**8a**) with Cp = η-C_5H_5 and M = Fe (ferrocene, **a**) or M = Co^+ (cobaltocenium, **b**). All compounds were characterized by elemental analysis, MS, IR, electrochemistry, Mössbauer spectroscopy (**a** only) and NMR spectroscopy. Solid state structures of **4a**, **6a**, **7a**, **3b**, and **5b** were determined by single crystal X-ray diffraction. ^{1}H NMR data (δ(NH) and $\Delta\delta$(NH) with T) as well as solution IR spectra were evaluated in order to determine intramolecular hydrogen bond interactions in solution. No intramolecular hydrogen bonds form in the monosubstituted derivatives **3**–**5** and in **8a**. For **7**, a strong intramolecular hydrogen bond is observed between the NH_{Ala} and CO_{Ala}, of the other ring, forming an 11-membered ring in solution as well as in the solid state. The situation is most complex for **6**, which forms an intramolecular 8-membered ring by hydrogen bonds $NH_{Phe} \cdots CO_{Cp}$ in the solid state (**6a**), but a symmetrical 11-membered ring structure with $NH_{Phe} \cdots CO_{Phe}$, bonds in solution. A comparison of the uncharged ferrocene derivatives with the iso-structural but positively charged cobaltocenium derivatives reveals only minor differences. Apparently, the presence of a positive charge does not significantly influence hydrogen bonds in peptide turn structures. Our results are related to geometries and amino acid sequences in protein turn structures and a nomenclature for turn mimetics with a *parallel* orientation of the two peptide strands is proposed.

Introduction

α-Helices and β-sheets are important secondary structural elements in peptides.[1] Extended structures are formed from these primary elements resulting in helix bundles or extended sheets. In particular, β-turns induce an extended sheet structure from two consecutive β-sheets, typically in an anti-parallel fashion. β-Turns and extended β-sheets are stabilized by hydrogen bonds. This structural motif has important implications for the biological function.[2] Consequently, β-turns have become target structures for medicinal research and a number of β-turn mimetics based on rigid organic molecules were designed.[3,4] Ferrocene derivatives were proposed as an organometallic scaffold for β-turns. In 1996, Herrick *et al*. reported compounds of the general type $Fe(C_5H_4$-CO-Xaa-OMe$)_2$ (with Xaa = amino acid) to have an ordered structure in organic solvents such as CH_2Cl_2 and $CHCl_3$.[5] This ordered structure is stabilized by two symmetrically equivalent hydrogen bonds between the amide NH and the methyl ester carbonyl moiety of another strand (Scheme 1). Because the inter-ring separation of ferrocene of about 3.3 Å is close to the N ··· O distance in β-sheets, this ordered conformation is a mimic for this secondary structural element. More recently, Hirao and co-workers prepared several disubstituted dipeptide derivatives, which contain a similar ordered structure.[6–9]

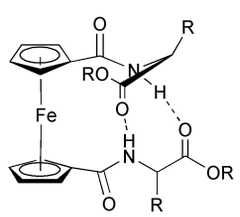

Scheme 1

Compared to purely organic scaffolds, ferrocene derivatives offer very favourable redox properties which were used in other types of molecular receptors.[10] Although the electrochemical reversibility of ferrocene oxidation is excellent under almost all circumstances, the one-electron oxidized ferrocenium compounds are generally not readily isolated and studied, especially in protic media. This precludes studies on the influence of charge on the structure and stability of β-turn mimetics based on ferrocene.

In this work, we present a series of novel cobaltocenium organometallic β-turn mimetics. Cobaltocenium derivatives are structurally very similar to ferrocene compounds, but the stable 18-electron form naturally possesses a positive charge.[11] A comparison to the iso-structural, but neutral, ferrocene derivatives makes it possible to assess the influence of charge on structure and stability of β-turns. In addition, a number of amine and peptide derivatives were synthesized where only some but not all of the hydrogen bonds that would stabilize a β-turn can form and their properties were investigated and compared to the full organometallic turn mimetics.

Experimental

All reactions were carried out in ordinary glassware and solvents. Chemicals were obtained from Aldrich or from Novabiochem. Enantiomerically pure L-amino acids were used. The dipeptide Boc-Ala-Phe-OMe was prepared according to

† Dedicated to Professor Wolfgang Beck, Ludwig-Maximilians-Universität München, on the occasion of his 70th birthday.

DOI: 10.1039/b208363a

standard peptide chemistry techniques from Boc-Ala-OH and H-Phe-OMe·HCl, employing isobutylchloroformate as the coupling reagent.[12] The Boc-protecting group of the dipeptide was removed by reaction with CH_2Cl_2/CF_3CO_2H (1 : 1, v/v) for 1 h at room temperature, followed by removal of the solvent *in vacuo*, yielding the dipeptide H-Ala-Phe-OMe·CF_3CO_2H as a white hygroscopic solid. The compounds $[Co(Cp)(C_5H_4\text{-}CO_2H)]PF_6$ (**1b**, Cp = η-C_5H_5) and $[Co(C_5H_4\text{-}CO_2H)_2]PF_6$ (**2b**) were synthesised according to literature methods.[13]

Elemental analyses were performed by H. Kolbe, Microanalytisches Laboratorium, Mülheim an der Ruhr, Germany. Infrared spectra were recorded on a Perkin-Elmer FT-IR spectrophotometer 2000 as KBr disks and/or in CH_2Cl_2 solution, with a spectral resolution of 4.0 cm^{-1}. Mass spectra were recorded on a Finnigan MAT 8200 instrument (EI, 70 eV) or on a Hewlett-Packard HP 5989 mass spectrometer (ESI and HR-MS; solvent and detection mode are given in parentheses). Cyclic voltammograms (CV) and square wave voltammograms (SWV) were recorded in CH_2Cl_2, with NBu_4PF_6 as supporting electrolyte, by using an EG&G Potentiostat/Galvanostat 273A. A three-electrode cell was employed with a glassy-carbon working electrode, a platinum wire auxiliary electrode and a Ag/$AgNO_3$ reference electrode (0.01 M $AgNO_3$ in MeCN). For determination of the redox potentials, ferrocene was added as an internal standard. ^{57}Fe Mössbauer spectra were recorded on an Oxford Instruments Mössbauer spectrometer in the constant acceleration mode, by using ^{57}Co/Rh as the radiation source. The measurements were performed at 80 K on solid samples containing a natural abundance of ^{57}Fe. The minimum experimental line-width was 0.24 mm s^{-1}. Isomer shifts were determined relative to α-Fe at 300 K. ^{1}H and ^{13}C NMR spectra were recorded on Bruker ARX 250 (^{1}H at 250.13 MHz), Bruker DRX 400 (^{1}H at 400.13 MHz) and Bruker DRX 500 (^{1}H at 500.35 MHz) instruments. ^{1}H and ^{13}C NMR spectra were referenced to TMS, using the ^{13}C or residual protio signals of the deuterated solvents as internal standards ($CDCl_3$ ≡ 7.24 (^{1}H) and 77.0 (^{13}C), DMSO ≡ 2.49 (^{1}H) and 39.5 (^{13}C)). Variable temperature ^{1}H NMR spectra were recorded on the Bruker DRX 400 NMR spectrometer. For these VT NMR experiments, $CDCl_3$ was dried over activated molecular sieves (3 Å) and the NMR tubes were thoroughly dried before use. High performance liquid chromatography (HPLC) purifications were performed by using a Macherey & Nagel Nucleosil 7-C-18 column (250 × 21 mm). As an eluent a 3 : 1 (v/v) mixture of MeCN and H_2O, the latter containing 0.05 mol L^{-1} $NaPF_6$ was used.

General synthesis of the ferrocene derivatives

Ferrocene carboxylic acid **1a** (230 mg, 1 mmol) or 1,1′-ferrocene dicarboxylic acid **2a** (274 mg, 1 mmol) were dissolved in DMF (15 mL) and NEt_3 (1.5 mL, 1.09 g, 10.8 mmol) was added. To this mixture were added stoichiometric amounts (*i.e.* 1 mmol for the synthesis of **3a**–**5a** and 2 mmol for the synthesis of **6a**–**8a**) of phenylalanine methyl ester hydrochloride (for **3a** and **6a**), *S*-1-phenylethylamine (for **5a** and **8a**) or the dipeptide H-Ala-Phe-OMe·CF_3CO_2H (for **4a** and **7a**). After addition of stoichiometric amounts of TBTU (*O*-(1*H*-benzotriazol-1-yl)-*N*,*N*,*N*′,*N*′-tetramethyluronium tetrafluoroborate, 1 mmol for **3a**, **4a** and **5a**; 2 mmol for **6a**, **7a** and **8a**), the mixture was stirred for 30 minutes at room temperature and subsequently evaporated to dryness *in vacuo*. The residue was suspended in CH_2Cl_2 (150 mL) and filtered to remove insoluble material, followed by washing of the CH_2Cl_2 solution with 2 M aqueous $NaHCO_3$ (100 mL), 1 M HCl (100 mL) and water (100 mL). The organic phase was dried over $MgSO_4$, filtered and evaporated to dryness under reduced pressure to yield an orange solid. Only in the case of **5a** and **8a** it was necessary to purify this solid by column chromatography over silica by using ethyl acetate–hexane (3 : 1, v/v) as the eluent. The first orange coloured band that eluted was the desired compound. Yields were 0.34 g (87%) for **3a**, 0.34 g (74%) for **4a**, 0.21 g (63%) for **5a**, 0.46 g (77%) for **6a**, 0.57 g (77%) for **7a**, and 0.25 g (52%) for **8a**. Crystals suitable for X-ray analysis of **6a** were grown by pentane diffusion into an ethyl acetate solution at room temperature. X-Ray quality crystals of **4a**·0.25CH_2Cl_2 were grown by slow evaporation of a CH_2Cl_2–hexane solution, whereas crystals suitable for X-ray structure determination of **7a**·0.5$CHCl_3$ were obtained by slow evaporation of a $CHCl_3$–heptane solution.

Fe(Cp)(η-C_5H_4-CO-Phe-OMe) (3a). ^{1}H NMR (400.13 MHz; $CDCl_3$; 293 K; 2 × 10^{-2} M): δ 7.32 (2H, mult, H_{Ar}), 7.26 (1H, mult, H_{Ar}), 7.18 (2H, mult, H_{Ar}), 6.00 (1H, br, NH), 5.01 (1H, mult, $C_\alpha H$), 4.62 (1H, H_{Cp}), 4.59 (1H, H_{Cp}), 4.33 (2H, H_{Cp}), 4.12 (5H, s, H_{Cp}), 3.76 (3H, s, OCH_3), 3.20 (1H, mult, $C_\beta H$), 3.14 (1H, mult, $C_\beta H$). ^{13}C NMR (100.6 MHz; $CDCl_3$): δ 172.3 ($C{=}O_{ester}$), 170.0 ($C{=}O_{amide}$), 136.1 ($C_{Ar,\ Phe}$), 129.2 ($C_{Ar,\ Phe}$), 128.7 ($C_{Ar,\ Phe}$), 127.2 ($C_{Ar,\ Phe}$), 75.3 ($C_{Cp,\ q}$), 70.5 (C_{Cp}), 69.7 (5C, C_{Cp}), 68.3, 68.0 (C_{Cp}), 52.8 (C_α), 52.3 (OCH_3), 38.0 (C_β). IR (KBr): 3299 (w, sh), 3266 (m, br, ν_{NH}), 1756 (s), 1736 (s, $\nu_{C=O,\ ester}$), 1631 (s), 1620 cm^{-1} (s, $\nu_{C=O,\ amide}$); IR (CH_2Cl_2): 3426 (w, ν_{NH}), 1741 (s, $\nu_{C=O,\ ester}$), 1659 cm^{-1} (s, $\nu_{C=O,\ amide}$). MS (EI): *m*/*z* = 391 (100) $[M]^+$, 331 (2) $[M - Cp]^+$, 213 (45). Anal. calc. for $C_{21}H_{21}NO_3Fe$ (391.25 g mol^{-1}): C, 64.47; H, 5.41; N, 3.58. Found: C, 64.41; H, 5.53; N, 3.64%.

Fe(Cp)(η-C_5H_4-CO-Ala-Phe-OMe) (4a). ^{1}H NMR (400.13 MHz; $CDCl_3$; 293 K; 2 × 10^{-2} M): δ 7.21 (3H, mult, H_{Ar}), 7.07 (2H, mult, H_{Ar}), 6.53 (1H, d, $^3J_{HH}$ = 7.8 Hz, NH_{Ala}), 6.18 (1H, d, $^3J_{HH}$ = 7.5 Hz, NH_{Phe}), 4.83 (1H, mult, $C_{\alpha,\ Phe}H$), 4.68 (1H, H_{Cp}), 4.63 (1H, H_{Cp}), 4.59 (1H, mult, $C_{\alpha,\ Ala}H$), 4.35 (2H, H_{Cp}), 4.17 (5H, s, H_{Cp}), 3.71 (3H, s, OCH_3), 3.13 (1H, mult, $C_{\beta,\ Phe}H$), 3.07 (1H, mult, $C_{\beta,\ Phe}H$), 1.41 (3H, d, *J* = 7.0 Hz, $CH_{3,\ Ala}$). ^{13}C NMR (100.6 MHz; $CDCl_3$): δ = 172.3 (br), 171.5 (C=O, only two resonances of C=O carbon atoms were observed), 135.6 ($C_{Ar,\ q}$), 129.4 (C_{Ar}), 128.6 (C_{Ar}), 126.9 (C_{Ar}), 74.9 ($C_{Cp,\ q}$), 70.8, 70.7, 69.2, 68.8 (all C_{Cp}), 70.1 (5H, C_{Cp}), 53.4, 52.5 (OCH_3 + $C_{\alpha,\ Phe}$), 49.2 (br, $C_{\alpha,\ Ala}$), 38.1 ($C_{\beta,\ Phe}$), 19.6 (br, $CH_{3,\ Ala}$). IR (KBr): 3301 (m, br, ν_{NH}), 1746 (s, $\nu_{C=O,\ ester}$), 1654 (s), 1625 cm^{-1} (vs, $\nu_{C=O,\ amide}$); IR (CH_2Cl_2): 3424 (m, $\nu_{NH,\ Phe}$ + $\nu_{NH,\ Ala}$), 1744 (s, $\nu_{C=O,\ ester}$), 1683 (s), 1651 cm^{-1} (s, $\nu_{C=O,\ amide}$). MS (EI): *m*/*z* = 462 (100) $[M]^+$. Anal. calc. for $C_{24}FeH_{26}N_2O_4$ (462.33 g mol^{-1}): C, 62.35; H, 5.67; N, 6.06. Found: C, 62.19; H, 5.61; N, 6.05%.

Fe(Cp)(η-C_5H_4-CO-NH-CH(CH_3)-Ph) (5a). ^{1}H NMR (400.13 MHz; $CDCl_3$; 293 K; 2 × 10^{-2} M): δ 7.37 (4H, mult, H_{Ar}), 7.27 (1H, mult, H_{Ar}), 5.82 (1H, d, *J* = 7.6 Hz, NH), 5.28 (1H, mult, NCH), 4.67 (1H, pseudo-d, H_{Cp}), 4.61 (1H, pseudo-d, H_{Cp}), 4.31 (2H, pseudo-t, H_{Cp}), 4.11 (5H, s, H_{Cp}), 1.56 (3H, d, *J* = 6.9 Hz, CH_3). ^{13}C NMR (62.9 MHz; $CDCl_3$): δ 169.3 (C=O), 143.6 ($C_{Ar,\ q}$), 128.7, 126.2, 127.4, 76.0 ($C_{Cp,\ q}$), 70.4, 70.4, 68.4, 67.8 (all C_{Cp}), 69.2 (5C, C_{Cp}), 48.5 (CH), 21.7 (CH_3). IR (KBr): 3294 (w, br, ν_{NH}), 1621 cm^{-1} (s, $\nu_{C=O}$); IR (CH_2Cl_2): 3440 (w, ν_{NH}), 1654 cm^{-1} (s, $\nu_{C=O}$). MS (EI): *m*/*z* = 333 (100) $[M]^+$. Anal. calc. for $C_{19}FeH_{19}NO$ (333.21 g mol^{-1}): C, 68.49; H, 5.75; N, 4.20. Found: C, 67.86; H, 5.65; N, 4.11%.

Fe(η-C_5H_4-CO-Phe-OMe)$_2$ (6a). ^{1}H NMR (400.13 MHz; $CDCl_3$; 293 K; 1 × 10^{-2} M): δ 7.75 (2H, d, *J* = 8.4 Hz, NH), 7.29 (6H, mult, H_{Ar}), 7.21 (4H, mult, H_{Ar}), 5.06 (2H, mult, $C_\alpha H$) 4.78 (2H, pseudo-t, H_{Cp}), 4.66 (2H, pseudo-t, H_{Cp}), 4.49 (2H, pseudo-t, H_{Cp}), 4.28 (2H, pseudo-t, H_{Cp}), 3.84 (6H, s, OCH_3), 3.18 (2H, mult, $C_\beta H$), 2.95 (2H, mult, $C_\beta H$). ^{13}C NMR ($CDCl_3$; 100.6 MHz): δ 175.4 ($C{=}O_{ester}$), 170.3 ($C{=}O_{amide}$), 136.7, 128.9, 128.6, 127.0 (all $C_{Ar,\ Phe}$), 75.9 ($C_{Cp,\ q}$), 71.9, 71.3, 70.4, 70.0 (all C_{Cp}), 54.0 (C_α), 52.8 (O–CH_3), 37.0 (C_β). IR (KBr): 3284 (w), 3219 (w, ν_{NH}), 1759 (m), 1740 (s, $\nu_{C=O,\ ester}$), 1630 cm^{-1} (s, $\nu_{C=O,\ amide}$); IR (CH_2Cl_2): 3380 (w, ν_{NH}), 1729 (s, $\nu_{C=O,\ ester}$), 1652 cm^{-1} (s, $\nu_{C=O,\ amide}$). MS (EI): *m*/*z* = 596 (100) $[M]^+$, 326 (15) $[M -$

CpCONPhe-OMe]$^+$. Anal. calc. for $C_{32}FeH_{32}N_2O_6$ (596.46 g mol^{-1}): C, 64.44; H, 5.41; N, 4.70. Found: C, 64.44; H, 5.51; N, 4.62%.

Fe(η-C_5H_4-CO-Ala-Phe-OMe)$_2$ (7a). ^{1}H NMR (400.13 MHz; $CDCl_3$; 293 K; 1×10^{-2} M): δ 8.33 (2H, d, J = 7.1 Hz, NH_{Ala}), 7.32 (4H, mult, H_{Ar}), 7.27 (2H, mult, H_{Ar}), 7.20 (4H, mult, H_{Ar}), 6.31 (2H, d, J = 7.7 Hz, NH_{Phe}), 4.88 (2H, H_{Cp}), 4.84 (2H, mult, $C_{\alpha,\ Phe}H$), 4.81 (2H, H_{Cp}), 4.61 (2H, mult, $C_{\alpha,\ Ala}H$) 4.46 (2H, H_{Cp}), 4.29 (2H, H_{Cp}), 3.66 (6H, s, OCH_3), 3.19 (2H, mult, $C_{\beta,\ Phe}H$), 3.16 (2H, mult, $C_{\beta,\ Phe}H$), 1.33 (6H, d, J = 7.1 Hz, $CH_{3,\ Ala}$). ^{13}C NMR (100.6 MHz; $CDCl_3$): δ 174.5 ($C{=}O_{ester}$), 171.6, 170.4 (br, C=O), 135.5 ($C_{Ar,\ q}$), 129.5, 128.6, 127.1 (all C_{Ar}), 75.6 ($_{CCp,\ q}$), 72.0, 71.3, 70.5, 70.4 (all C_{Cp}), 53.9, 52.3 (OCH_3 + $C_{\alpha,\ Phe}$), 49.5 (br, $C_{\alpha,\ Ala}$), 37.9 ($C_{\beta,\ Phe}$), 17.5 (br, $CH_{3,\ Ala}$). IR (KBr): 3277 (m, br, ν_{NH}), 1750 (s, $\nu_{C=O,\ ester}$), 1669 (s), 1625 cm^{-1} (s, $\nu_{C=O,\ amide}$); IR (CH_2Cl_2): 3414 (m, $\nu_{NH,\ Phe}$), 3322 (m, $\nu_{NH,\ Ala}$), 1744 (s, $\nu_{C=O,\ ester}$), 1677 (s), 1644 cm^{-1} (s, $\nu_{C=O,\ amide}$). MS (EI): m/z = 738 (100) [M]$^+$. Anal. calc. for $C_{38}FeH_{42}N_4O_8$ (738.62 g mol^{-1}): C, 61.79; H, 5.73; N, 7.59. Found: C, 61.57; H, 5.78; N, 7.65%.

Fe(η-C_5H_4-CO-NH-CH(CH_3)-Ph)$_2$ (8a). ^{1}H NMR (400.13 MHz; $CDCl_3$; 293 K; 1×10^{-2} M): δ 7.42 (4H, mult, H_{Ar}), 7.34 (4H, mult, H_{Ar}), 7.25 (2H, mult, H_{Ar}), 6.93 (2H, d, J = 7.9 Hz, NH), 5.25 (2H, mult, N–CH), 4.45 (2H, pseudo-t, H_{Cp}), 4.32 (2H, pseudo-t, H_{Cp}), 4.24 (2H, pseudo-t, H_{Cp}), 4.21 (2H, mult, H_{Cp}), 1.61 (6H, d, J = 7.0 Hz, both CH_3). ^{13}C NMR (62.9 MHz; $CDCl_3$): δ 169.3 (C=O), 143.9 ($C_{Ar,\ q}$), 128.5, 126.4, 127.2, 78.2 ($C_{Cp,\ q}$), 72.3, 71.1, 70.7, 69.2 (all C_{Cp}), 49.2 (CH), 21.9 (CH_3). IR (KBr): 3392 (w), 3382 (m, ν_{NH}), 1637 cm^{-1} (s, $\nu_{C=O}$); IR (CH_2Cl_2): 3435 (w, ν_{NH}), 1638 cm^{-1} (s, $\nu_{C=O}$). MS (EI): m/z = 480 (100) [M]$^+$, 268 (10) [M − Cp-CO-NH-CH(CH_3)-Ph]. Anal. calc. for $C_{28}FeH_{28}N_2O_2$ (480.39 g mol^{-1}): C, 70.01; H, 5.87; N, 5.83. Found: C, 68.37; H, 6.08; N, 5.68%.

General synthesis of the monsubstituted cobaltocenium complexes

To a solution of [Co(Cp)(C_5H_4-CO_2H)]PF_6 **1b** (379 mg, 1.0 mmol) in DMF (10 mL) was added NEt_3 (1.0 mL, 0.73 g, 7 mmol) and TBTU (323 mg, 1.0 mmol) and either phenylalanine methyl ester hydrochloride (216 mg, 1.0 mmol, for **3b**) or H-Ala-Phe-OMe·CF_3CO_2H (1 mmol, 364 mg, for **4b**). The mixture was stirrred for 30 min and subsequently evaporated to dryness *in vacuo*. The residue was suspended in CH_2Cl_2 (100 mL) and filtered to remove insoluble material. The resulting clear yellow solution was washed with 2 M $NaHCO_3$ (50 mL), 1 M HCl (50 mL) and water (50 mL). The CH_2Cl_2 was dried over $MgSO_4$ and subsequently removed under reduced pressure, yielding a sticky yellow residue. This was dissolved in MeOH (10 mL), followed by addition of a $NaBPh_4$ (0.25 g, 0.73 mmol) solution in MeOH (10 mL). Upon standing overnight, a yellow precipitate formed, which was isolated by filtration and washed with MeOH (5 mL) and air dried. Yields were 0.26 g (36%) for **3b** and 0.10 g (13%) for **4b**. X-Ray quality crystals of **3b** were grown by slow evaporation of a MeOH solution.

[Co(Cp)(C_5H_4-CO-Phe-OMe)]BPh_4 (3b). ^{1}H NMR (400.13 MHz; $CDCl_3$; 293 K; 2×10^{-2} M): δ 7.48 (8H, mult, H_{Ar}), 7.30 (2H, mult, H_{Ar}), 7.15 (2H, mult, H_{Ar}), 7.05 (8H, mult, H_{Ar}), 6.90 (5H, mult, H_{Ar}), 6.11 (1H, d, J = 7.9 Hz, NH), 4.99 (2H, app. s, H_{Cp}), 4.85 (2H, app. s, H_{Cp}), 4.80 (5H, s, H_{Cp}), 4.54 (2H, app. s, H_{Cp}), 4.50 (2H, app. s, H_{Cp}), 3.77 (3H, s, OCH_3), 3.28 (1H, mult, $C_\beta H$), 3.06 (1H, mult, $C_\beta H$). ^{13}C NMR (125.8 MHz; CD_3OD): δ 173.1 ($C{=}O_{ester}$), 165.3 (q, $^2J_{BC}$ = 49 Hz, $C_{q,\ Ph}$), 163.8 ($C{=}O_{amide}$), 138.5 ($C_{Ar,\ Phe,\ q}$), 137.3 ($C_{Ar,\ Ph}$), 130.1 ($C_{Ar,\ Phe}$), 129.8 ($C_{Ar,\ Phe}$), 128.2 ($C_{Ar,\ Phe}$), 126.4 ($C_{Ar,\ Ph}$), 122.7 ($C_{Ar,\ Ph}$), 94.1 ($C_{Cp,\ q}$), 87.4 (C_{Cp}), 87.3 (5C, C_{Cp}), 85.3 (C_{Cp}), 85.0 (C_{Cp}), 55.5 (C_α), 53.1 (O–CH_3), 37.7 (C_β). IR (KBr): 3404 (w, ν_{NH}), 1735 (s, $\nu_{C=O,\ ester}$), 1674 cm^{-1} (s, $\nu_{C=O,\ amide}$); IR (CH_2Cl_2): 3403 (w, ν_{NH}), 1744 (s, $\nu_{C=O,\ ester}$), 1654 cm^{-1} (s, $\nu_{C=O,\ amide}$). MS (ESI-pos.; CH_3OH): m/z = 394 [**3b**-BPh_4]$^+$. Anal. calc. for $BC_{45}CoH_{41}NO_3$ (713.57 g mol^{-1}): C, 75.74; H, 5.75; N, 1.96. Found: C, 75.58; H, 5.74; N, 2.01%.

[Co(Cp)(C_5H_4-CO-Ala-Phe-OMe)]BPh_4 (4b). ^{1}H NMR (400.13 MHz; DMSO-d_6): δ 8.69 (1H, d, J = 6.9 Hz, NH), 8.53 (1H, d, J = 7.1 Hz, NH), 7.26 (13H, mult, H_{Ar}), 6.93 (8H, mult, H_{Ar}), 6.79 (4H, mult, H_{Ar}), 6.40 (1H, H_{Cp}), 6.24 (1H, H_{Cp}), 5.86 (2H, pseudo-d, H_{Cp}), 5.79 (5H, s, H_{Cp}), 3.58 (3H, s, OCH_3), $C_{\alpha,\ Ala}H$ obscured by the H_2O signal, 3.02 (2H, mult, $C_{\beta,\ Phe}H$), 1.35 (3H, d, J = 7.0 Hz, $CH_{3,\ Ala}$). ^{13}C NMR (100.6 MHz; DMSO-d_6): δ 172.21, 171.9 (C=O), 163.3 (q, $^2J_{BC}$ = 49 Hz, $C_{q,\ Ph}$), 137.1 ($C_{q,\ Phe}$), 135.5 ($C_{Ar,\ Ph}$), 129.1, 128.3, 126.6 (all $C_{Ar,\ Phe}$), 125.3, 121.5 (both $C_{Ar,\ Ph}$), 92.6 ($C_{Cp,\ q}$), 86.0, 85.7, 84.5, 83.6 (all C_{Cp}), 86.0 (5C, C_{Cp}), 53.9, 51.4 (OCH_3 + $C_{\alpha,\ Phe}$), 36.5 ($C_{\beta,\ Phe}$), 17.5 ($CH_{3,\ Ala}$). IR (KBr): 3416 (m), 3381 (w, ν_{NH}), 1724 (s, $\nu_{C=O,\ ester}$), 1679 cm^{-1} (vs, $\nu_{C=O,\ amide}$). MS (ESI-pos; MeOH): m/z = 465 [**4b** − BPh_4]$^+$. Anal. calc. for $BC_{48}H_{46}CoN_2O_4$ (784.65 g mol^{-1}): C, 73.48; H, 5.91; N, 3.57. Found: C, 73.33; H, 5.86; N, 3.61%.

Synthesis of [Co(Cp)(C_5H_4-CO-*S*-NH-CH(CH_3)-Ph)$_2$]BPh_4 (5b). This compound was prepared analogously as described for the other mono-substituted cobaltocenium compounds **3b** and **4b** by using *S*-1-phenylethylamine. After addition of a methanolic $NaBPh_4$ solution, about 10 mg of X-ray quality crystals separated the first time the synthesis was performed. The X-ray crystal structure confirms the identity of this compound. However, it could not be reproduced because when tried again, the precipitate that formed upon addition of $NaBPh_4$ was found to be contaminated with *S*-1-phenylethylammonium salts, which were not readily removed. $BC_{43}CoH_{39}NO$ (655.5 g mol^{-1}). Anal. calc. C, 78.79; H, 6.00; N, 2.14. Found: C, 76.32; H, 5.82; N, 2.06%. IR (KBr): 3384m (ν_{NH}), 1667s ($\nu_{C=O}$) cm^{-1}. MS (ESI-pos., MeOH): m/z = 336 [**5b** − BPh_4]$^+$.

General synthesis of the disubstituted cobaltocenium complexes

To a solution of [Co(C_5H_4-CO_2H)$_2$]PF_6 **2b** (217 mg, 0.5 mmol) in DMF (6 mL) was added NEt_3 (1.0 mL, 0.73 g, 7 mmol) and *O*-(1*H*-benzotriazol-1-yl)-*N*,*N*,*N*′,*N*′-tetramethyluronium hexafluorophosphate (HBTU, 182 mg, 0.5 mmol) and either phenylalanine methyl ester hydrochloride (216 mg, 1.0 mmol, for **6b**) or H-Ala-Phe-OMe·CF_3CO_2H (1 mmol, 364 mg, for **7b**). The mixture was stirrred for 30 minutes and subsequently evaporated to dryness *in vacuo*. The residue was suspended in CH_2Cl_2 (100 mL) and filtered to remove insoluble material. The resulting clear yellow solution was washed with 2 M $NaHCO_3$ (50 mL), 1 M HCl (50 mL) and water (50 mL). The CH_2Cl_2 was dried over $MgSO_4$ and subsequently removed under reduced pressure. The resulting sticky residue was dried for several hours *in vacuo*, yielding a hygroscopic yellow foam-like solid. This solid was purified by preparative HPLC, employing a 3 : 1 mixture of MeCN and H_2O (the latter containing 0.05 M $NaPF_6$) as the eluent. The work-up consisted of concentration of the eluent to about a quarter of its volume under reduced pressure. The remaining solution was extracted with CH_2Cl_2 (3 × 50 mL) and the CH_2Cl_2 was dried over $MgSO_4$. Removal of the CH_2Cl_2 *in vacuo* afforded the desired compounds in highly pure form. Yield: 110 mg (32%) for **6b** and 50 mg (11%) for **7b**.

[Co(C_5H_4-Phe-OMe)$_2$]PF_6 (6b). ^{1}H NMR (400.13 MHz; $CDCl_3$; 293 K; 1×10^{-2} M): δ 7.79 (2H, d, J = 8.3 Hz, NH), 7.33 (6H, mult, H_{Ar}), 7.25 (2H, mult, H_{Ar}), 6.12 (2H, pseudo-t, H_{Cp}), 5.82 (6H, mult, H_{Cp}), 3.83 (6H, s, OCH_3), 3.35 (2H, mult, $C_\beta H$), 3.05 (2H, mult, $C_\beta H$). ^{13}C NMR ($CDCl_3$; 100.6 MHz): δ 171.8 ($C{=}O_{ester}$), 162.2 ($C{=}O_{amide}$), 137.2 ($C_{Ar,\ q}$), 129.2, 128.5, 127.4 (all C_{Ar}), 92.9 ($C_{Cp,\ q}$) 88.2, 87.3, 86.6, 84.9 (all C_{Cp}), 54.9 (C_α), 52.6 (OCH_3), 36.3 (C_β). IR (KBr): 3216 (m, br, ν_{NH}), 1742 (s, $\nu_{C=O,\ ester}$), 1670 cm^{-1} (s, $\nu_{C=O,\ amide}$); IR (CH_2Cl_2): 3403 (w), 3362 (w, ν_{NH}), 1743 (s), 1721 cm^{-1} (s, $\nu_{C=O,\ ester}$). MS (ESI-pos.; MeOH):

m/*z* = 599 [**6b** − PF_6]$^+$. Anal. calc. for $C_{32}CoF_6H_{32}N_2O_6P$ (744.51 g mol^{-1}): C, 51.62; H, 4.33; N, 3.76. Found: C, 51.46; H, 4.40; N, 3.72%.

[Co(C_5H_4-Ala-Phe-OMe)$_2$]PF_6 (7b). ^{1}H NMR (400.13 MHz; $CDCl_3$; 5 × 10^{-3} M; 293 K): δ 8.79 (2H, d, J = 6.4 Hz, NH_{Ala}), 7.32 (4H, mult, H_{Ar}), 7.28 (2H, mult, H_{Ar}), 7.22 (4H, mult, H_{Ar}), 6.57 (2H, br, NH), 6.32 (2H, br, H_{Cp}), 6.26 (2H, br, H_{Cp}), 6.02 (2H, br, H_{Cp}), 5.87 (2H, br, H_{Cp}), 4.83 (2H, mult, $C_{\alpha,\ Phe}H$), 4.57 (2H, mult, $C_{\alpha,\ Ala}H$), 3.70 (s, 6H, OCH_3), 3.16 (4H, mult, $C_{\beta,\ Phe}H$), 1.36 (6H, d, J = 7.4 Hz, $CH_{3,\ Ala}$). ^{13}C NMR (62.9 MHz; $CDCl_3$): δ 173.7 ($C{=}O_{ester}$), 171.6 ($C{=}O_{Ala}$), 161.2 ($C{=}O_{Cp}$), 135.9 ($C_{Ar,\ q}$), 129.3, 128.6, 127.1 (all C_{Ar}), 92.1 ($C_{Cp,\ q}$), 87.9, 87.5, 86.0, 85.4 (all C_{Cp}), 54.0, 52.4 (OCH_3 and $C_{\alpha,\ Phe}$), 49.9 ($C_{\alpha,\ Ala}$), 37.6 ($C_{\beta,\ Phe}$), 16.9 ($CH_{3,\ Ala}$). IR (CH_2Cl_2): 3405 (w, $\nu_{NH,\ Phe}$), 3296 (w, $\nu_{NH,\ Ala}$), 1744 (s, $\nu_{C=O,\ ester}$), 1660 cm^{-1} (s, $\nu_{C=O,\ amide}$). MS (ESI-pos.; MeOH): *m*/*z* = 741 [**7b** − PF_6]$^+$; exact mass: 741.2332; $C_{38}CoH_{42}N_4O_8$ requires 741.2335.

X-Ray crystallographic data collection and refinement of the structures

Yellow single crystals of **3b**, **5b**, **7a**, and yellow brownish crystals of **4a** and **6a** were coated with perfluoropolyether. Suitable crystals were picked up with a glass fiber and were immediately mounted in the nitrogen cold stream of the diffractometer to prevent the loss of solvent. Intensity data were collected at 100 K using graphite monochromated Mo-Kα radiation (λ = 0.71073 Å). Final cell constants were obtained from a least squares fit of a subset of several thousand strong reflections. Data collection was performed by hemisphere runs taking frames at 0.3° (Siemens SMART, **4a**, **5b** and **6a**) and 0.5° (Nonius Kappa-CCD, **3b** and **7a**) in ω. A semiempirical absorption correction using the program SADABS[14] was performed on the data sets of **4a**, **5b**, **6a**. The program DelRefAbs which is part of the PLATON99[15] program suite was used to account for absorption of a crystal needle of **7a** since data redundancy was not sufficient for a semiempirical correction. Intensity data of **3b** were not corrected.

The ShelXTL software package[16] was used for solution, refinement and artwork of the structure. The structures were readily solved by direct methods and difference Fourier techniques. Absolute structure parameters were checked by refining the inverse structure and are reliable. Solvent molecules in **4a** and **7a** were found to be disordered and not fully occupied. A split atom model with restrained C–Cl and Cl–Cl distances and a reduced occupancy factor satisfactorily described the disorder of the chloroform molecule in **7a**. The occupancy factor of the CH_2Cl_2 molecule in **4a** was reduced to 0.25 and C–Cl distances were restrained to be equal within a certain error. All non-hydrogen atoms, except C atoms in disordered solvent molecules, were refined anisotropically. Hydrogen atoms were placed at calculated positions and refined as riding atoms with isotropic displacement parameters. Crystallographic data of the compounds are collected in Table 1.

CCDC reference numbers 180589–180593.

See http://www.rsc.org/suppdata/dt/b2/b208363a/ for crystallographic data in CIF or other electronic format.

Results and discussion

Synthesis

The synthesis and constitution of the ferrocene derivatives are depicted in Schemes 2 and 3. The ferrocene compounds (**a**) were synthesised by reacting ferrocene mono- (**1a**) or 1,1′-di-carboxylic acid (**2a**) with stoichiometric amounts of *S*-1-phenylethylamine (PEA), *S*-phenylalanine methyl ester or the dipeptide H-Ala-Phe-OMe in DMF in the presence of equimolar amounts of the coupling reagent *O*-(1*H*-benzotriazol-1-yl)-*N*,*N*,*N*′,*N*′-tetramethyluronium tetrafluoroborate (TBTU) and excess NEt_3. After work-up, the compounds were obtained as orange solids. Only in the case of the *S*-1-phenylethylamine derivatives **5a** and **8a**, an extra purification step by column chromatography over silica was necessary because small amounts of unreacted amine were found to be present in the isolated solids. Yields varied from 52 to 87%. Compounds **3a** and **6a** have been reported before, but were not fully characterised.[5,17]

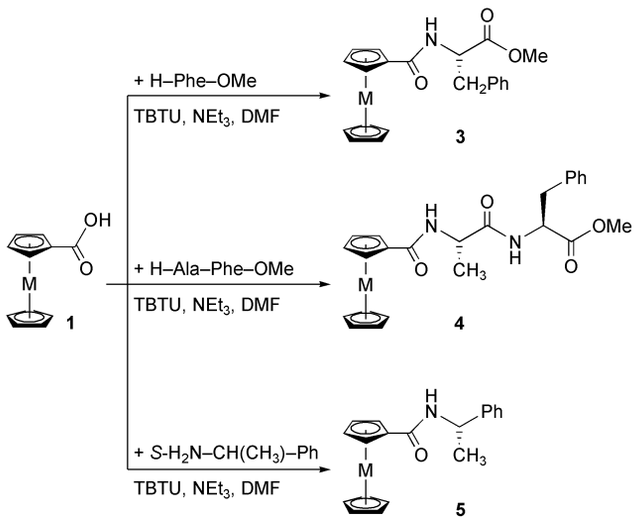

Scheme 2

The synthesis and constitution of the cobaltocenium compounds (**b**) are also depicted in Schemes 2 and 3. The cobaltocenium acids (mono-, **1b**, or 1,1′-di, **2b**) are, in contrast to their ferrocene analogues, not commercially available and were synthesised according to a published procedure.[13] The first part of the synthesis of the mono cobaltocenium derivatives **3b** and **4b** was performed analogously to that of the ferrocene derivatives, but oily residues were obtained after the extractive work-up and removal of the solvent. After dissolution in MeOH and addition of a $NaBPh_4$ solution in methanol, the compounds precipitated in pure form as their tetraphenylborate salts. The yield of the cobaltocenium compounds **3b** and **4b** was lower than of their ferrocene analogues. This may be attributed to the overall positive charge of the cobaltocenium complexes, which makes them more water-soluble, resulting in significant losses during extractive work-up.

The di-substituted cobaltocenium derivatives **6b** and **7b** were obtained by reacting cobaltocenium di-carboxylic acid **2b** with either H-Phe-OMe or H-Ala-Phe-OMe in DMF with TBTU as the coupling reagent. After extractive work-up, the oily residue was dried *in vacuo* for a few hours, yielding the compounds as hygroscopic powders, with purity around 90–95% as concluded from their ^{1}H NMR spectra. Unfortunately, the complexes could not be purified by crystallisation and also did not precipitate from MeOH upon addition of anions which are unable to act as hydrogen bond acceptors, such as BF_4^- and tetraphenylborate. Instead, analytically pure samples were obtained by preparative HPLC purification (see Materials and methods).

Our interest also concerned the *S*-1-phenylethylamine cobaltocenium derivatives. However, the work-up of the reaction of [Co(C_5H_4-CO_2H)$_2$]PF_6 with two equivalents of *S*-1-phenylethylamine did not proceed smoothly, because the organic layer was invariably colourless after the washing steps. Also the mono *S*-1-phenylethylamine derivative **5b** was difficult to obtain. By using an identical procedure as for the compounds **3b** and **4b**, a small amount of X-ray quality crystals of [Co(Cp)(C_5H_4-CO-*S*-NH-CH(CH_3)-Ph)]BPh_4 (**5b**) was obtained. However, when tried again, the precipitates were contaminated

Table 1 Summary of crystallographic data for **6a**, **4a**·0.25CH_2Cl_2, **7a**·0.5$CHCl_3$, **3b** and **5b**

	6a	**4a**·0.25CH_2Cl_2	**7a**·0.5$CHCl_3$	**3b**	**5b**
Chemical formula	$C_{32}H_{32}FeN_2O_6$	$C_{24}H_{26}FeN_2O_4$·0.25CH_2Cl_2	$C_{38}H_{42}FeN_4O_8$·0.5$CHCl_3$	$C_{45}H_{41}BCoNO_3$	$C_{43}H_{39}BCoNO$
FW	596.45	483.55	798.29	713.53	655.49
Crystal size/mm	0.53 × 0.18 × 0.18	1.28 × 0.70 × 0.60	0.60 × 0.18 × 0.12	0.36 × 0.22 × 0.10	0.50 × 0.38 × 0.08
Crystal system	Hexagonal	Tetragonal	Monoclinic	Orthorhombic	Triclinic
Space group	$P6_5$	$P4_32_12$	$P2_1$	$P2_12_12$	$P1$
a/Å	22.332(2)	17.2236(14)	12.7711(8)	13.992(2)	9.493(1)
b/Å	22.332(2)	17.2236(14)	16.4209(10)	39.148(7)	9.925(1)
c/Å	10.3690(7)	16.9834(12)	18.269(12)	13.195(2)	9.947(1)
α/°	90	90	90	90	97.90(3)
β/°	90	90	93.44(1)	90	92.80(3)
γ/°	120	90	90	90	115.51(3)
V/Å^3	4478.4(5)	5038.2(7)	3824(3)	7228(2)	831.7(2)
Z	6	8	4	8	1
D (calcd.), g/cm^3	1.327	1.275	1.386	1.311	1.309
T/K	100(2)	100(2)	100(2)	100(2)	100(2)
λ/Å	0.71073	0.71073	0.71073	0.71073	0.71073
Absorption coefficient/mm^{-1}	0.551	0.682	0.556	0.518	0.552
$R1$ [$I > 2\sigma(I)$][a]	0.0532	0.0703	0.0516	0.0713	0.0434
$wR2$ (all data)[b]	0.1567	0.2124	0.1551	0.1480	0.0942
Data/restraints/parameters	4974 /1/372	9122/2/300	14096/31/986	11283/0/919	5814/3/427
GooF on F^2[c]	1.039	1.079	1.022	0.922	1.014
Flack parameter	−0.01(2)	0.02(2)	−0.012(14)	0.02(2)	0.022(11)

[a] $R1 = \Sigma||F_o| - |F_c||/\Sigma|F_o|$. [b] $wR2 = [\Sigma[w(F_o^2 - F_c^2)^2]/\Sigma[w(F_o^2)_2]]^{1/2}$, where $w = 1/\sigma^2(F_o^2) + (aP)^2 + bP$, $P = (F_o^2 + 2F_c^2)/3$. [c] GooF = $[\Sigma[w(F_o^2 - F_c^2)^2]/(n - p)]^{1/2}$ where n = no. of reflections and p = no. of refined parameters.

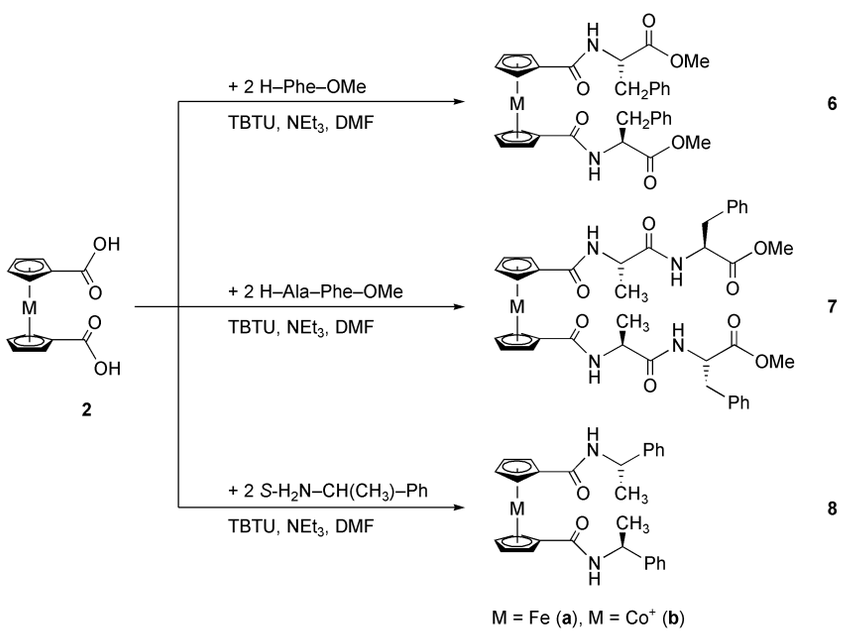

Scheme 3

with *S*-1-phenylethylammonium salts. Since the corresponding cobaltocenium di-*S*-phenylethylamine derivative **8b** could not be obtained at all, the purification as well as the total characterisation of **5b** was not pursued further.

S-1-Phenylethylamine (PEA) appears to be much less reactive towards coupling reactions with the organometallic acids than amino acids or dipeptides. The disubstituted PEA cobaltocenium derivative could not be obtained at all, and also the yield for the other PEA compounds is significantly lower compared to the amino acid or dipeptide derivatives.

Solid state structures

In order to determine intramolecular hydrogen bonding interactions, the X-ray single crystal structures of **4a**·0.25CH_2Cl_2, **6a**, **7a**·0.5$CHCl_3$, **3b** and **5b** were determined. Details on how the crystals were obtained are given in the Materials and methods section. In this discussion, no metal–C(Cp) bond distances will be presented because none of these values is exceptional and they show only statistical variations between the structures presented. However, a number of more elusive structural parameters, such as the tilt and other specific angles will be presented below (see Table 2 and Scheme 4).

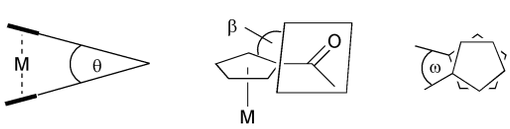

Scheme 4

An ORTEP projection for the cationic part of [Co(Cp)(C_5H_4-CO-*S*-NH-CH(CH_3)-Ph)]BPh_4 (**5b**) is shown in Fig. 1. The cation does not display any unusual structural features, and the unit cell consists of an isolated complex cation and a tetraphenylborate anion. Hydrogen bonds are not present in the solid state. This is consistent with the observation of the amide

Table 2 Summary of specific angles (°) for the X-ray crystal structures[a]

Angle[a]	**6a**	**4a**·0.25CH_2Cl_2	**7a**·0.5$CHCl_3$[b]		**3b**[b]		**5b**
θ[c]	4.7	1.1	1.3	1.5	3.3	1.9	0.7
β[d]	31.4/15.1[e]	6.1	4.1/5.8[e]	3.7/10.3[e]	10.5	9.9	5.5
ω[f]	68.9		70.3	68.9			

[a] Angles are visualised in Scheme 4. [b] Two independent molecules in the unit cell; first value(s) correspond(s) to molecule A. [c] The dihedral angle between the two Cp rings. [d] The dihedral angle between the plane of the Cp ring and the C(*ipso*)-C=O bond. [e] Disubstituted derivatives; first value for β corresponds to the C=O moiety with the lower atomic label. [f] The torsion angle is defined as C(*ipso*)–Cp(centroid)–Cp(centroid)–C(*ipso*).

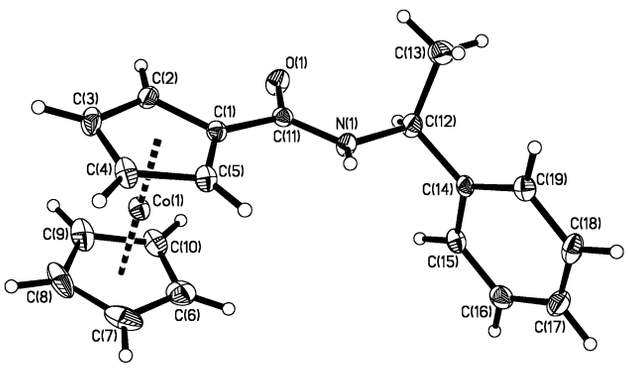

Fig. 1 ORTEP plot of the cation of **5b**. Thermal ellipsoids are depicted at 50% probability.

ν_{NH} stretch vibration at 3384 cm^{-1} in the infrared spectrum of **5b** as a KBr pellet.

The unit cell of **3b** consists of two crystallographically independent complex cations and two tetraphenylborate anions. ORTEP diagrams of both cations are depicted in Fig. 2. In cation A (left) the phenyl ring of the phenylalanine substituent is directed towards the unsubstituted Cp-ring and the methyl ester is pointing downwards. In cation B (right) on the other hand, the substituents have more or less exchanged positions relative to cation A, *i.e.* the phenyl ring is located away from the substituted Cp-ring and the methyl ester is directed towards the unsubstituted Cp-ring.[18] No hydrogen bonds are present in the solid state, which is consistent with the observation of the amide ν_{NH} stretch vibration at 3404 cm^{-1} in the infrared spectrum of **3b** (KBr).

An ORTEP plot for the asymmetric unit in **6a** is shown in Fig. 3. The compound crystallises in the hexagonal space group $P6_5$, which implies the presence of a left-handed six-fold screw axis in the unit-cell. The molecules are arranged in a helical fashion around this six-fold screw axis, linked together *via* intermolecular hydrogen bond interactions between N(27) and O(6) of another molecule (N ··· O contact 2.935 Å). The structure is stabilized by an intramolecular hydrogen bond between N(7) and O(26) (N ··· O contact 2.832 Å). The helix has a pitch of 10.3690(7) Å, which is equivalent to the length of the crystallographic *c*-axis. Per definition, the six-fold screw axis is aligned parallel to this axis in the hexagonal space group $P6_5$.

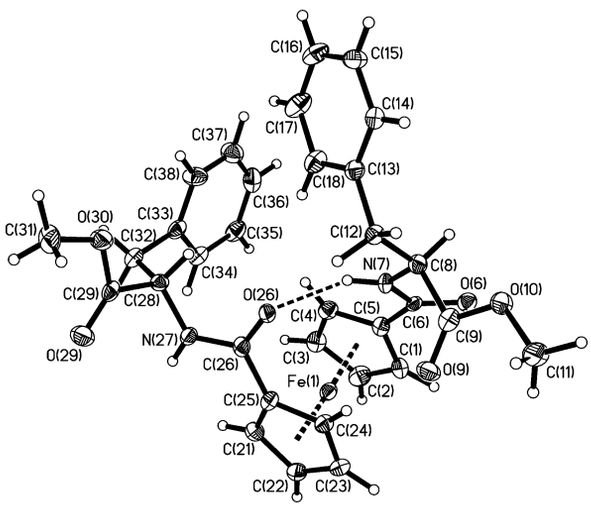

Fig. 3 ORTEP plot of the asymmetric unit of **6a**. Thermal ellipsoids are depicted at 50% probability.

The X-ray crystal structure of a different bis-amino acid methyl ester ferrocene derivative, namely Fe(C_5H_4-CO-Val-OMe)$_2$, has been reported.[19] This valine derivative has the ordered conformation depicted in Scheme 1 in the solid state and shows two very weak symmetry-related hydrogen bond interactions between the amide NH group and the methyl ester carbonyl oxygen atom with N ··· O contacts of 3.247 Å. In contrast to Fe(C_5H_4-CO-Val-OMe)$_2$, **6a** does not have intramolecular hydrogen bonds between the ester carbonyl oxygen atom and the amide NH moiety. Apparently, the presence of bulky phenyl rings in **6a** compared to the smaller iso-propyl side chains in Fe(C_5H_4-CO-Val-OMe)$_2$ induces a different packing in the solid state. The crystal structure of another bis-amino acid ferrocene derivative with C-terminal amide protecting groups, namely Fe(C_5H_4-CO-Gly-NH_2)$_2$ has been reported as well.[20] Like Fe(C_5H_4-CO-Val-OMe)$_2$, this glycinamide compound has the ordered conformation shown in Scheme 1, with N ··· O contacts of 2.88 Å. The shorter N ··· O contacts for Fe(C_5H_4-CO-Gly-NH_2)$_2$ compared to Fe(C_5H_4-CO-Val-OMe)$_2$ are attributed to the better hydrogen acceptor properties of amide carbonyl oxygen atoms compared to methyl ester carbonyl oxygen atoms.

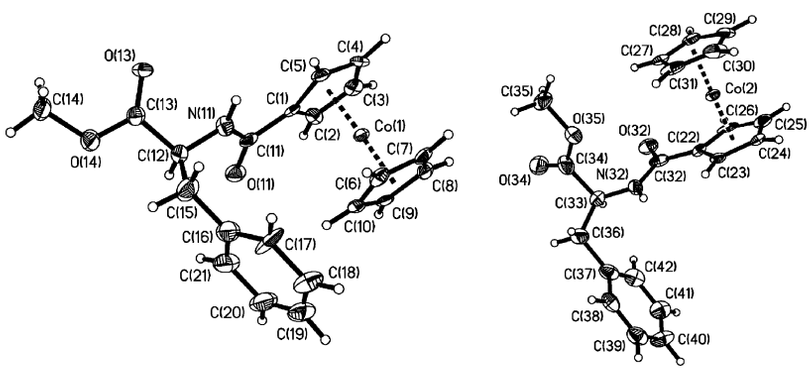

Fig. 2 ORTEP plot of the two independent cations of **3b** (A: left and B: right). Thermal ellipsoids are depicted at 50% probability.

An ORTEP representation for the asymmetric unit of **4a**·$0.25CH_2Cl_2$ is shown in Fig. 4. The compound crystallises in the

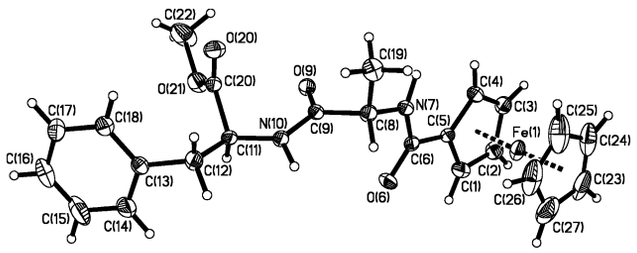

Fig. 4 ORTEP plot of the asymmetric unit of **4a**. Thermal ellipsoids are depicted at 50% probability.

tetragonal space group $P4_32_12$, which implies the presence of a left-handed four-fold screw axis in the unit cell. The molecules are arranged in a helical fashion around this screw axis, as shown in Fig. 5. Intermolecular hydrogen bond interactions are present between N(7) and O(6) of a neighbouring molecule (N ··· O contact 2.936 Å) and between N(10) and O(9) of the same neighbouring molecule (N ··· O contact 2.862 Å).

The helix has a pitch of 16.9834(12) Å, which is equal to the length of the crystallographic *c*-axis, and a helical rise of 4.0 units. This type of helix is very interesting, because two hydrogen bond donors and two acceptors exist per molecule. Three other ferrocenyl dipeptides have been structurally characterised by X-ray crystallography, namely Fe(Cp)(C_5H_4-CO-Pro-Pro-OBzl),[21] Fe(Cp)(C_5H_4-CO-Gly-Pro-OEt)[9] and Fe(Cp)(C_5H_4-CO-Ala-Pro-OEt).[6] All these compounds contain at least one Pro residue which cannot form amide hydrogen bonds. Consequently, hydrogen bonding is different compared to **4a**, with the compounds Fe(Cp)(C_5H_4-CO-Ala-Pro-OEt) and Fe(Cp)-(C_5H_4-CO-Gly-Pro-OEt) showing a zigzag hydrogen bonding arrangement, and of course no hydrogen bonds are present in the case of Fc(Cp)(C_5H_4-CO-Pro-Pro-OBzl) due to the absence of amide NH groups. We have recently observed a zigzag orientation induced by intermolecular hydrogen bonding in ferrocene alkyne derivatives.[22]

X-Ray crystallography revealed the presence of two crystallographically independent molecules in the unit cell of **7a**·$0.5CHCl_3$, which display only slightly different bond lengths and angles. An ORTEP diagram for one of the crystallographically independent molecules is depicted in Fig. 6. There

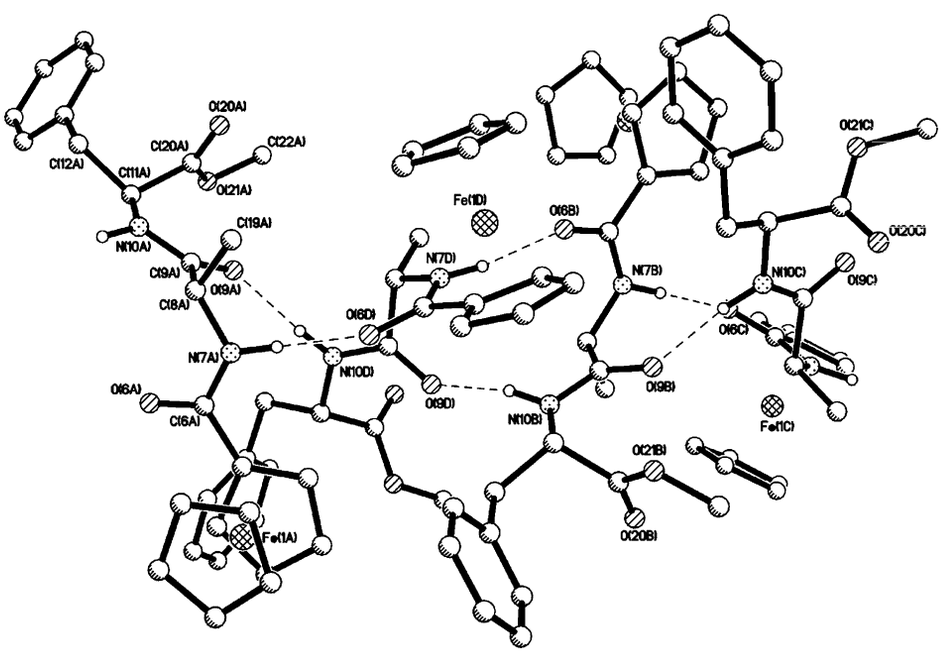

Fig. 5 Packing diagram for **4a**, indicating intermolecular hydrogen bond interactions and visualizing the helical arrangement of the molecules.

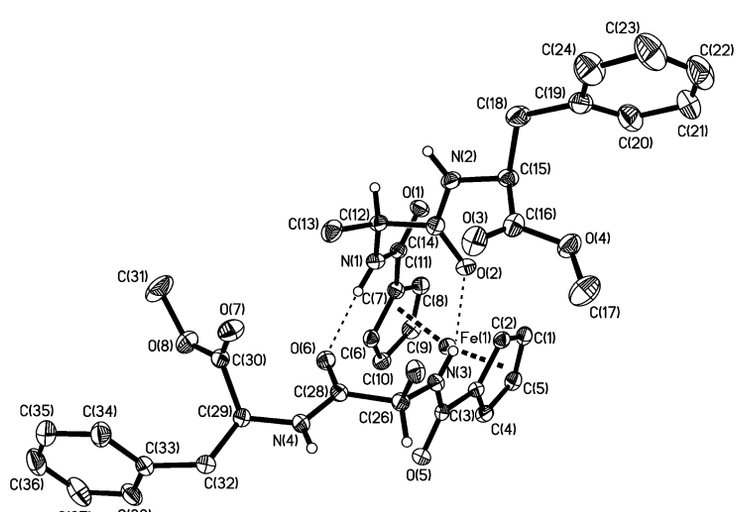

Fig. 6 ORTEP plot of one of the crystallographically independent molecules of **7a**. All geometrical parameters of the second independent molecule are very similar. Thermal ellipsoids are depicted at 50% probability.

are two intramolecular hydrogen bonds between the alanine NH group and the alanine carbonyl moiety of the other strand. In molecule A (depicted in Fig. 6), the N ··· O contacts are 2.921 and 2.924 Å (N(1) ··· O(6) and N(3) ··· O(2), respectively), whereas these N ··· O contacts are slightly shorter in the other independent molecule (molecule B, not depicted, 2.901 and 2.893 Å).

In addition to intramolecular hydrogen bonds, there are also intermolecular hydrogen bond interactions between the phenylalanine NH groups and the ferrocenyl C=O moieties of two neighbouring molecules that belong to the same crystallographic type. Each dipeptide strand forms intermolecular hydrogen bonds to a different molecule of the same type, resulting in infinite chains of molecules A and B throughout the lattice. Between molecules A, the N ··· O contacts are 2.834 and 2.844 Å (N(4) ··· O(1) and N(2) ··· O(5), respectively), whereas they are 2.830 and 2.836 Å for the intermolecular hydrogen bonds between molecules B. The hydrogen bonds are arranged in such way that a 14-membered ring forms, as visualised in Fig. 7. A similar arrangement has recently been

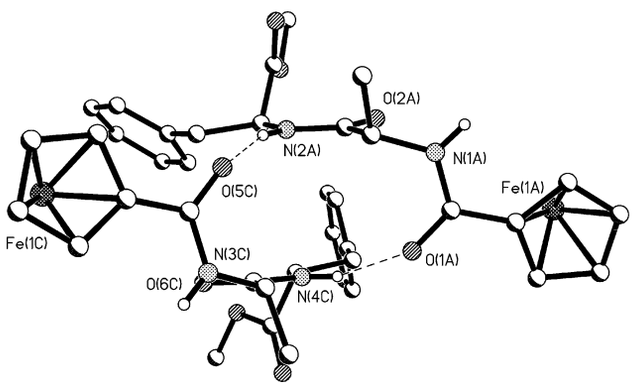

Fig. 7 Visualisation of the 14-membered ring that forms *via* intermolecular hydrogen bonds between two molecules of **7a**.

observed for the packing of $Fe(C_5H_4$-CO-Gly-Phe-OMe$)_2$.[8] In contrast to this compound, the unit cell of **7a** contains two crystallographically independent molecules.

Structural parameters for the five X-ray crystal structures are summarised in Table 2, and the corresponding angles are visualised in Scheme 4. The Cp rings in all structures are almost coplanar. The largest deviation from coplanarity is observed for **6a**. The tilt of 4.7° in **6a** is likely due to the rigid hydrogen bonded helical arrangement of the complex molecules. This deviation is slightly larger than what is usually observed for disubstituted ferrocenes bearing carboxyl substituents.[23,24] For comparison, a large value of 16.4° for θ was reported for an imine-bridged [3]ferrocenophane.[25]

The amide moieties in all structures, except in **6a**, are almost coplanar with the Cp-rings ($\beta \approx 0$), resulting in a maximum π-overlap between the cyclopentadienyl and amide π systems. The large β angle for **6a** of 31.4° is due to the intramolecular hydrogen bond interaction, which forces one of the amide moieties to rotate significantly out of the Cp plane. Because of a cosine dependence, an angle of 31.4° still corresponds to about 86% of the maximum overlap between the amide π orbitals and the cyclopentadienyl π system.[26] This deviation from planarity of the amide functionality in **6a** is not exceptional: twists of 45.7 and even 50.2° have been observed previously for constrained disubstituted ferrocene compounds.[25,27]

The observed ω angles for **6a** and both independent molecules of **7a** are close to the ideal value for a 1,2′-conformation (360/5 = 72°). Similar ω values were found for Fe(Cp-CO-Ala-Pro-OR$)_2$ (R = Me, Et or Bzl) and several other disubstituted ferrocenes that are part of a macrocycle.[7,23] The substituted Cp rings of these derivatives are forced into this 1,2′-conformation either by intramolecular hydrogen bonds or by steric constraints of the rigid macrocycle. In the case of difunctionalised ferrocenes without such constraints, the substituents will be arranged in such way as to minimize steric interactions. Consequently, ω angles much larger than 80° are observed for disubstituted ferrocene derivatives of that type.

Table 3 Summary of spectroscopic data for the NH hydrogen atoms in **3a**–**7b**

Compound	ν_{NH} [a]	δNH [b]	$^3J_{HH}$ [c]	$\Delta\delta$ [d]
3a	3436 [e]	6.00 [e]	n.r.[h,i]	−1.4
4a	3424 [e]	6.53 [e]	7.8	−5.4
		6.18	7.5	−3.6
5a	3440 [e]	5.82 [e]	7.6	−2.2
6a	3380 [f]	7.75 [f]	8.4	−5.2
7a	3322 [f]	8.33 [f]	7.1	−4.5
	3414	6.31	7.7	−2.4
8a	3435 [f]	6.93 [f]	7.9	−7.2
3b	3404 [e]	6.11 [e]	7.9	−0.7
4b	3404 [g]	n.d.[n]	n.d.[n]	n.d.[n]
6b	3362 [f]	7.79 [m]	8.3	−8.6
	3403 [k]			
7b	3296 [f]	8.82	6.8	−4.7
	3405	6.58	n.r.[h,i]	n.r.[h,o]

[a] In cm^{-1}; in CH_2Cl_2. [b] In dry $CDCl_3$; T = 293 K; in ppm. [c] In Hz. [d] Temperature range: 223–323 K; in ppb K^{-1}. [e] 2×10^{-2} M. [f] 1×10^{-2} M. [g] 5×10^{-3} M. [h] n.r. = not reliable. [i] Broad NH resonance observed. [k] Second ν_{NH} vibration observed. See text for explanation. [m] Value not reliable because the complex is very hygroscopic. [n] Insoluble in $CDCl_3$. [o] Resonance becomes very broad at T < 293 K.

Solution structures

Although solid state structures provide reliable and accurate data about the molecular constitution, the molecular conformation in solution is decisive for biological function. Hydrogen bonds in the turn region determine the stability and biological function of β-turns. It was therefore crucial to investigate the presence and strength, at least qualitatively, for the β-turn mimetics under investigation in this study. To this end, at least two spectroscopic techniques have been established, namely infrared and ^{1}H NMR spectroscopy. Amide NH hydrogen atoms that are not hydrogen bonded display ν_{NH} stretch vibrations in the infrared spectrum at wavenumbers higher than 3400 cm^{-1} and show resonances in between 5.5 and 7.0 ppm in the ^{1}H NMR spectrum in solvents which themselves do not form hydrogen bonds, such as $CDCl_3$ or CD_2Cl_2. NH stretching vibrations below 3400 cm^{-1} in the infrared spectrum are diagnostic of hydrogen bonded amide NH hydrogen atoms.[28,29] In addition, amide NH hydrogen atoms involved in hydrogen bond interactions have a chemical shift higher than 7.5 ppm. The temperature dependence $\Delta\delta^1$H of the amide proton resonance is another criterium. Small values of $\Delta\delta^1$H between −2 to −4 ppb K^{-1} are diagnostic for amide protons which are either not hydrogen bonded at all or fixed in a very strong locked hydrogen bond. Peptide amide protons in a dynamic hydrogen bond produce larger effects.[30]

Relevant infrared and ^{1}H NMR spectroscopic data for **3a**–**7b** are summarised in Table 3. The mono-substituted ferrocenes **3a**, **4a** and **5a** and cobaltocenium complexes **3b** and **4b** display ν_{NH} stretching vibrations at wavenumbers higher than 3400 cm^{-1} and chemical shifts of the NH hydrogen atoms between 5.8 and 6.5 ppm in $CDCl_3$ (Table 3). This indicates that the NH hydrogen atoms of these compounds do not form hydrogen bonds in solution, as expected and observed previously for **3a**[5] and several other mono substituted ferrocene amino acid and dipeptide conjugates.[6–9]

The ferrocene di-phenylalanine methyl ester derivative **6a** shows a ν_{NH} stretch vibration at 3380 cm^{-1} and a chemical shift of 7.75 ppm for the NH hydrogen atoms.[5] In the case of the

di-*S*-1-phenylethylamine derivative **8a**, the ν_{NH} stretch vibration is located at 3435 cm^{-1} and the NH hydrogen atom resonates at 6.93 ppm. The differences between **6a** and **8a** can only be explained by the presence of two intramolecular hydrogen bonds between the amide NH and the methyl ester carbonyl moiety in **6a**. Because there is no ester group in **8a**, no hydrogen bonds can form. The differences between the mono PEA derivative **5a** and its disubstituted analogue **8a** is small, suggesting that only weak hydrogen bonds of **8a** exist in solution. If the amide group twists to a small extent out of the Cp-plane, a weak hydrogen bond may be possible between the amide NH and the amide C=O of the other Cp-ring. The resulting decrease in resonance energy between the planar Cp-ring and the planar amide is compensated by the hydrogen bond interaction at least to a certain extent. For the solid state structure of **6a** a rotation of the amide C=O moiety out of the Cp plane has been observed crystallographically.

In the case of the di-substituted Ala-Phe-OMe ferrocene **7a** the hydrogen bond observed in the solid state between the Ala-NH group and the Ala-C=O moiety of the other strand is also present in solution. This can be derived from the position of the ν_{NH} stretch vibration at 3322 cm^{-1} and the chemical shift of this NH hydrogen atom, which is located at 8.33 ppm. This hydrogen bond in **7a** is stronger than the one in the di-Phe-OMe derivative **6a**, which is consistent with the differences between the hydrogen bond acceptor strengths of ester and amide carbonyl moieties. The ν_{NH} stretch vibration at 3322 cm^{-1} is in the range reported for several other disubstituted ferrocene derivatives bearing dipeptide substituents.[6–9]

The phenylalanine NH hydrogen atom is not involved in any hydrogen bond interactions, as concluded from a ν_{NH} stretch vibration at 3414 cm^{-1} and the chemical shift of 6.31 ppm. The resonances of these alanine and phenylalanine amide NH hydrogen atoms were assigned unambiguously by 2D NMR techniques. Only the first NH hydrogen atom can form an intramolecular hydrogen bond in solution, whereas the second cannot because of spatial reasons, similar to what is observed for the X-ray crystal structure of **7a**.[8,9]

The disubstituted cobaltocenium Ala-Phe-OMe derivative **7b** has a conformation in solution identical to that of the ferrocene analogue **7a**, with the alanine NH moieties of this compound being involved in two intramolecular hydrogen bonds. The ν_{NH} stretch vibration of the alanine NH group in **7b** is observed about 25 cm^{-1} lower in energy compared to **7a**. However, this may be an intrinsic property of the charged cobaltocenium derivatives, because the ν_{NH} stretching vibrations of the mono-substituted derivatives **3b** and **4b** are also about 20–30 cm^{-1} lower than those for the corresponding ferrocene derivatives **3a** and **4a**. The chemical shift of the alanine NH hydrogen atom in **7b** is shifted significantly to higher field compared to that of the ferrocene analogue **7a** (8.82 ppm in **7b** *vs.* 8.33 ppm in **7a**). The chemical shift difference between the NH hydrogen atoms in **3a** and **3b** is significantly smaller (0.11 ppm). This value probably reflects the intrinsic difference between uncharged ferrocene and charged cobaltocenium amides. A much larger difference between the resonances of the alanine NH hydrogen atoms in **7b** and **7a** then seems to indicate a stronger hydrogen bond in the cobaltocenium derivative **7b**.[31]

The disubstituted Phe-OMe cobaltocenium derivative **6b** displays two amide NH stretching vibrations in the infrared spectrum. The vibration at 3362 cm^{-1} is assigned as the NH vibration of the hydrogen bonded NH moiety and the one at 3403 cm^{-1} is assigned to an NH stretching vibration originating from a non-hydrogen bonded NH.[28] In fact, the latter value is identical to that of the mono phenylalanine derivative **3b**, which cannot be involved in any intramolecular hydrogen bond interactions at all.

Coupling constants $^3J(C_\alpha H–NH)$ are important to determine the conformation of a peptide in solution.[32] The values of the coupling constants for the compounds **3a**–**7b** between 6.8 and 8.4 Hz are not very informative, because they indicate dihedral angles ϕ of around 90°,[33] which is a standard value for a *trans*-configured amide.

Variable temperature measurements over a range of about 100 K were made to investigate the temperature dependence $\Delta\delta^1H$ of the amide NH hydrogen atoms (Table 3). $\Delta\delta^1H$ values between −2 to −4 ppb K^{-1} are generally considered diagnostic for amide NH hydrogen atoms that are either locked in a very strong hydrogen bond or not hydrogen bonded at all.[30] Values outside this range were associated with moderately strong hydrogen bonds. The temperature dependence is explained by reversible formation of the hydrogen bond, a process which is evidently strongly influenced by temperature. However, no quantitative expression that correlates $\Delta\delta^1H$ with the strength of a hydrogen bond has been derived yet and this criterion is basically used in a qualitative way. $\Delta\delta^1H$ values are tabulated in Table 3. Although a trend in those values seems to prevail, they are unfortunately not unambiguous. In compound **7a**, two different values of −4.5 and −2.4 ppb K^{-1} are observed. This is in accordance with IR and δ^1H_{NH} data which suggest that the first amide proton is hydrogen bonded, whereas the second is not. Likewise, large negative values are observed for compounds **6a**, **6b** and one proton of **7b**, all of which do presumably form intramolecular hydrogen bonds. On the other hand, a large negative value of −7.2 ppb K^{-1} for **8a** seems to suggest a hydrogen bond, which is at odds with IR and δ^1H data. Likewise, hydrogen bonds are not expected for compound **4a**, leaving the $\Delta\delta^1H$ value of −5.4 ppb K^{-1} unexplained.[34]

Table 4 Reversible one-electron transitions for **3a**–**7b**[a]

Compound	$E_{1/2}$[b]	Compound	$E_{1/2}$[b]
3a	+0.19	**6a**	+0.40
4a	+0.19	**7a**	+0.34
5a	+0.17	**8a**	+0.35
$[Co(Cp)_2]PF_6$	−1.36[c]	$[Co(Cp)_2]PF_6$	−1.34[d]
3b	−1.13	**6b**	−0.93
4b	−1.13	**7b**	−1.00

[a] In CH_2Cl_2; NBu_4PF_6 as supporting electrolyte. [b] In V; *vs.* Fc/Fc^+. [c] Measured value in this work. [d] From ref. 44.

Electrochemistry

Redox potentials for the ferrocene and cobaltocenium derivatives are tabulated in Table 4. The substituted ferrocene derivatives display higher oxidation potentials than ferrocene itself (by definition 0.00 V). The increase of the oxidation potential upon substitution of the Cp ring by amide groups can be explained by the withdrawal of electron density from the ferrocene moiety by these substituents.[24,35] The substituent effects are roughly additive, with each amide group contributing about 180 mV. A similar type of behaviour of the redox potentials for mono and 1,1′-ferrocenes has been observed previously.[6,7,17,36] The size or nature of the substituent on ferrocene does not have a significant influence on the redox potentials. The variation of $E_{1/2}$ is certainly too small to differentiate between different substituents.[36]

There is a fundamental difference between the electrochemical behaviour of ferrocene derivatives and their isoelectronic cobaltocenium analogues in that the former can be oxidised to yield a 17-electron species, whereas the latter can only undergo a one-electron reduction to yield 19-electron compounds. Reduction potentials for the cobaltocenium derivatives **3b**–**7b** are shown in Table 4. From this table, it is observed that the reduction shifts to less negative potentials upon substitution of a Cp-ring with an amide moiety. If both Cp-rings are substituted, the shift of the reduction potential is significantly larger. This shows that the e_{1g} level is lowered in energy, or in other words, becomes more accessible if electron-

Table 5 ^{57}Fe Mössbauer spectroscopic data at 80 K for ferrocene and compounds **3a**–**8a**

Compound	δ^a	$\Delta E_Q{}^a$	Γ^a
$Fe(C_5H_5)_2$	0.53 [b]	2.42 [b]	
3a	0.53	2.37	0.34
4a	0.52	2.32	0.28
5a	0.53	2.32	0.30
6a	0.52	2.27	0.27
7a	0.52	2.27	0.32
8a	0.51	2.27	0.30

[a] In mm s^{-1}. [b] From ref. 38.

withdrawing substituents are present.[11,26,37] The direction of the observed shift upon substitution of a Cp-ring is the same as observed for the ferrocene derivatives.

^{57}Fe Mössbauer spectra

The results from ^{57}Fe Mössbauer spectroscopic investigations on **3a**–**8a** are summarized in Table 5. The isomer shifts for **3a**–**8a** are virtually identical to those of ferrocene.[38] However, they display a lower quadrupole splitting than ferrocene. The values for the quadrupole splitting of the disubstituted derivatives **6a**, **7a** and **8a** are significantly lower than those of the monosubstituted compounds **3a**, **4a** and **5a**. It has been noted before that the quadrupole splitting of ferrocene decreases upon substitution of a Cp ring with an electron-withdrawing substituent and even more when such a substituent is introduced on both Cp rings.[39] This effect can be explained by withdrawal of electron density from the orbital e_{1g}, the highest occupied orbital with Cp character.[11,26,37] This leads to a different field gradient along the molecular axis and, thus, to a different value for the quadrupole splitting.

Conclusions

In this work, we have prepared a number of di- and tetra-peptides with a metallocene backbone. The length of the peptide chains was systematically varied and the metal was switched between Fe and Co^+ to change the overall charge of the constructs. Both means were undertaken in order to investigate the position and possibly strength of hydrogen bonds. In each case, mono-substituted metallocene derivatives were compared to their 1,1′-disubstituted analogues. Evidence for strong intramolecular hydrogen bonding was found in derivatives **6** and **7**. Preliminary evidence for intramolecular hydrogen bonding was reported by Herrick *et al*. for bis(amino acid) ferrocene derivatives $Fc(CO\text{-}Xaa\text{-}OMe)_2$ (see Scheme 1).[5] An intramolecular hydrogen bond between amide NH and ester CO was suggested by those workers based on NMR and IR evidence and subsequently verified experimentally in two related X-ray single crystal structures.[19,20] In this work, we rather find an intramolecular hydrogen bond between the amide NH and ferrocene carbonyl CO for Xaa = Phe (**6a**) by X-ray crystallography. There is evidence for NH hydrogen bonding in solution for **6a**, although this interaction appears to be less strong than the one in the ferrocene bis(dipeptide) **7a**. To clarify this issue, we have prepared mono- and di-(*S*-1-phenylethylamine) ferrocene derivatives **5a** and **8a**. These compounds are similar in their steric requirements to **6a** but lack the ester group altogether. NMR and IR data are very similar for both compounds and give no indication for NH hydrogen bonds in either **5a** or **8a** in solution. In **7a**, on the other hand, a (strong) intramolecular NH ··· CO(amide) hydrogen bond is most likely present in solution as well as in the solid state. We conclude that in our compound **6a** *different* types of hydrogen bonds form in the solid state and in solution, namely NH ··· CO(amide) in the solid state as confirmed by X-ray analysis and NH ··· CO(ester) in solution. This behaviour is in contrast to the previously reported compounds[5,19,20] and underscores the need for structural investigations in solution as well as in the solid state.

The peptides with an organometallic scaffold in this work were designed such as to mimic structural properties in peptides, in particular turn structures. A typical turn structure is depicted schematically in Scheme 5. Ring constraints by

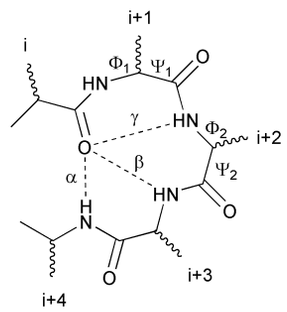

Scheme 5

hydrogen bonds define γ-turns (7-membered ring) or β-turns (10-membered rings), whereas 13-membered rings are present in α-helices.[2] A classification of different β-turn geometries was introduced by Venkatachalam depending on the angles Φ_n and Ψ_n.[40] Before and after the turn, the peptide extends as anti-parallel strands, often in β-sheets. The organometallic scaffolds used in this and previous work are diacids. As such, they enforce a parallel orientation of the peptide strands and may not seem "real" β-turn mimetics. Nevertheless, topological similarities remain which will be discussed below.

First of all, let us compare the solid state structures of **6a** and **7a**. In **6a**, an intramolecular hydrogen bond is formed between O26 and N7. If connecting atoms are counted (H7–N7–C6–C5–Fe1–C25–C26–O26), an 8-membered ring is formed. Carbonyl groups may be counted as follows: C26–O26 (i), C6–O6 (i + 1), then N7 is the amide nitrogen atom of the (i + 2) amino acid. The situation is different for **7a**. Two intramolecular hydrogen bonds N1 ··· O6 and N3 ··· O2 are formed. Both define 11-membered rings between O (i) and N (i + 3) if a procedure as for **6a** is applied. Because of the approximate C_2 symmetry of this molecule the same rules apply to either Cp ring and their substituents. Taking these data together, we conclude that the turn structure in **6a** is γ-turn-like, and the one found in **7a** is β-turn-like. Because of the parallel orientation induced by the diacid scaffold, we denote the turn structures pseudo-γ_p and pseudo-β_p.

Another important point is the overall charge of the turn structure. Following an analysis by Hutchinson and Thornton,[41] Asp is the only (negatively) charged amino acid that is frequently found in β-turns (in the i position). The two positively charged amino acids under physiological conditions (Lys and Arg) are not frequently encountered at all in this type of secondary structural element. This may seem astonishing in light of the fact that additional hydrogen bonds (*e.g*. of Ser) are indeed used to stabilize the turn structure. Furthermore, turn structures are frequently involved in molecular recognition of a protein by its receptor and are thus exposed to the (usually hydrophilic) surface of the protein. In this work, a comparison between uncharged ferrocene derivatives **6a** and **7a** and positively charged cobaltocenium derivatives **6b** and **7b** is presented. Both pairs of compounds do presumably form very similar structures as suggested by their analytical data. Indeed, none of the data differ enough to infer a substantial difference in either structure or strength of intramolecular hydrogen bonds in solution. Hence, our work underscores that a nearby positive charge does not influence hydrogen bonds that stabilize a turn structure significantly.

The positional preference of certain amino acids in β-turns in protein crystal structures has been studied by Thornton and co-workers.[41,42] To induce and stabilize a turn, Pro is the most common amino acid at the (i + 1) position (restriction of Φ to about −60°). In organometallic mimics like ferrocene or cobaltocene, a "turn-like" structure is inherent in the molecular geometry of the two Cp rings. Thus, no special amino acid is required to induce a turn. On the other hand, the two rings can rotate against each other and situate substituents in 1 and 1′ position of the two rings into virtually any torsion angle ω (see Table 2 and Scheme 4). As discussed above and shown in Table 2, an angle of about 70° is present in both **6a** and **7a**. Evidently, this is a favourable angle for turn structures and stabilized by hydrogen bonds, much like β- or γ-turns in proteins need additional stabilization through hydrogen bonds as visualized in Scheme 5.

The torsional flexibility discussed above is a unique property of the metallocene mimics proposed in this study. In comparison, most of the purely organic mimics are much more rigid.[4] The well-known phenoxathiine derivatives designed by Feigel and co-workers are a pivotal example in which rigidity is imposed by their tricyclic aromatic backbone.[43] Recent studies imply that some flexibility is indeed necessary for biological activity. Upon binding to the receptor, changes in the geometry of both the receptor and the small β-turn mimicking molecule take place that optimize interactions and thus bonding ("induced fit"). We believe that the torsional flexibility of the turn mimetics proposed in this paper may bear some relevance to the biological activity of β-turn mimetics with a metallocene backbone. Studies along these lines are in progress in the Heidelberg group.

Acknowledgements

The experimental part of this work was carried out at the Max-Planck-Institut für Strahlenchemie. The authors are grateful to the Max-Planck-Gesellschaft and Prof. K. Wieghardt for support of this work. We are grateful to J. Bitter and K. Sand for running numerous NMR spectra, H. Schucht for technical assistance with the X-ray determinations, B. Mienert for recording the Mößbauer spectra and M. Trinoga for HPLC services. N. M. N. would like to acknowledge financial support from the Fond der Chemischen Industrie and the Deutsche Forschungsgemeinschaft (DFG).

References and notes

1 L. Stryer, *Biochemistry*, W. H. Freeman and Company, San Francisco, 1994.
2 D. P. Fairlie, M. L. West and A. K. Wong, *Curr. Med. Chem.*, 1998, **5**, 29–62.
3 D. Obrecht, M. Altorfer and J. A. Robinson, *Adv. Med. Chem.*, 1999, **4**, 1–68.
4 G. Hölzemann, *Kontakte (Darmstadt)*, 1991, **1**, 3–13; G. Hölzemann, *Kontakte (Darmstadt)*, 1991, **2**, 55–64.
5 R. S. Herrick, R. M. Jarret, T. P. Curran, D. R. Dragoli, M. B. Flaherty, S. E. Lindyberg, R. A. Slate and L. C. Thornton, *Tetrahedron Lett.*, 1996, **37**, 5289–5292.
6 A. Nomoto, T. Moriuchi, S. Yamazaki, A. Ogawa and T. Hirao, *Chem. Commun.*, 1998, 1963–1964.
7 T. Moriuchi, A. Nomoto, K. Yoshida and T. Hirao, *J. Organomet. Chem.*, 1999, **589**, 50–58.
8 T. Moriuchi, A. Nomoto, K. Yoshida, A. Ogawa and T. Hirao, *J. Am. Chem. Soc.*, 2000, **123**, 68–75.
9 T. Moriuchi, A. Nomoto, K. Yoshida and T. Hirao, *Organometallics*, 2001, **20**, 1008–1013.
10 A. Togni and T. Hayashi, *Ferrocenes: Homogeneous Catalysis, Organic Synthesis, Material Science*, VCH, Weinheim, 1995.
11 N. J. Long, *Metallocenes*, Blackwell Science, Oxford, 1998.
12 J. Meienhofer, *The Mixed Carbonic Anhydride Method of Peptide Synthesis*, Academic Press, London, 1979.
13 J. E. Sheats and M. D. Rausch, *J. Org. Chem.*, 1970, **35**, 3245–3249.
14 G. M. Sheldrick, SADABS, University of Göttingen, 1994.
15 A. L. Spek, L. J. Farrugia, in PLATON99, Utrecht, 1999.
16 G. M. Sheldrick, ShelXTL, University of Göttingen, 1994.
17 W. Bauer, K. Polborn and W. Beck, *J. Organomet. Chem.*, 1999, **579**, 269–279.
18 D. R. van Staveren, T. Weyhermüller and N. Metzler-Nolte, *Organometallics*, 2000, **19**, 3730–3735.
19 M. Oberhoff, L. Duda, J. Karl, R. Mohr, G. Erker, R. Fröhlich and M. Grehl, *Organometallics*, 1996, **15**, 4005–4011.
20 A. S. Georgopoulou, D. M. P. Mingos, A. J. P. White, D. J. Williams, B. R. Horrocks and A. Houlton, *J. Chem. Soc., Dalton Trans.*, 2000, 2969–2974.
21 H. B. Kraatz, D. M. Leek, A. Houmam, G. D. Enright, J. Lusztyk and D. D. M. Wayner, *J. Organomet. Chem.*, 1999, **589**, 38–49.
22 O. Brosch, T. Weyhermüller and N. Metzler-Nolte, *Eur. J. Inorg. Chem.*, 2000, 323–330.
23 M. C. Grossel, M. R. Goldspink, J. A. Hriljac and S. C. Weston, *Organometallics*, 1991, **10**, 851–860.
24 L. Lin, A. Berces and H.-B. Kraatz, *J. Organomet. Chem.*, 1998, **556**, 11–20.
25 T. Moriuchi, I. Ikeda and T. Hirao, *Organometallics*, 1995, **14**, 3578–3580.
26 T. A. Albright, J. K. Burdett and M.-H. Whangbo, *Orbital Interactions in Chemistry*, John Wiley & Sons, New York, 1985.
27 C. D. Hall, I. P. Danks, S. C. Nyburg, A. W. Parkins and N. W. Sharpe, *Organometallics*, 1990, **9**, 1602–1607.
28 G.-B. Liang, G. P. Dado and S. H. Gellman, *J. Am. Chem. Soc.*, 1991, **113**, 3994–3995.
29 S. H. Gellman, G. P. Dado, G.-B. Liang and B. R. Adams, *J. Am. Chem. Soc.*, 1991, **113**, 1164–1173.
30 C. N. Kirsten and T. H. Schrader, *J. Am. Chem. Soc.*, 1997, **119**, 12061–12068.
31 Although every effort was made to work under stringent conditions, this result should be taken with appropriate care. Compound **7b** is very hygroscopic and the presence even of trace amounts of water would already influence the measurements significantly.
32 G. C. K. Roberts, in *NMR of Macromolecules – A Practical Approach*, ed. D. Rickwood, B. D. Hames, Oxford University Press, Oxford, 1993.
33 H. Günther, *NMR Spectroscopy*, John Wiley & Sons, New York, 1980.
34 Intermolecular interactions can be excluded and reliable $\Delta\delta^1$H values are obtained only if the concentration of the solution is lower than the self-association constant of the compound under investigation. This work was carried out on approximately 10 mM solutions, which is expected to be well beyond a self-association constant. However, the self-association concentrations were not determined and therefore, there is a slight chance that 10 mM solutions were already too concentrated at least in some cases. Furthermore, the presence of even small amounts of water is expected to influence the $\Delta\delta$ values to a large extent. Therefore, we feel that the presence and the strength of hydrogen bonds can be much better determined from the position of the ν_{NH} stretch vibration in the infrared spectrum and the chemical shift of the amide NH hydrogen atoms.
35 M. V. Baker, H.-B. Kraatz and J. W. Quail, *New J. Chem.*, 2001, **25**, 427–433.
36 H.-B. Kraatz, J. Lusztyk and G. D. Enright, *Inorg. Chem.*, 1997, **36**, 2400–2405.
37 A. Haaland, *Acc. Chem. Res.*, 1979, **12**, 415–422.
38 N. N. Greenwood and T. C. Gibb, *Mössbauer Spectroscopy*, Chapman and Hall, London, 1971.
39 R. M. G. Roberts and J. Silver, *J. Organomet. Chem.*, 1984, **263**, 235–241.
40 C. M. Venkatachalam, *Biopolym.*, 1968, **6**, 1425–1434.
41 E. G. Hutchinson and J. M. Thornton, *Protein Sci.*, 1994, **3**, 2207–2216.
42 C. M. Wilmot and J. M. Thornton, *J. Mol. Biol.*, 1988, **203**, 221–232.
43 M. Feigel, *J. Am. Chem. Soc.*, 1986, **108**, 181–182.
44 M.-H. Koepp, H. Wendt and H. Strehlow, *Z. Elektrochem., Ber. Bunsenges. Phys. Chem.*, 1960, **64**, 483.